Meteorol. Atmos. Phys. 45, 125–138 (1991)

Meteorology and Atmospheric Physics

551.513.1

Institut für Geophysik und Meteorologie, Universität zu Köln, Federal Republic of Germany

The Global Energy Cycle of Stationary and Transient Atmospheric Waves: Results from ECMWF Analyses

U. Ulbrich and **P. Speth**

With 15 Figures

Received February 2, 1990
Revised May 14, 1990

Summary

The role of stationary (monthly mean) and transient (departure from monthly mean) waves within the atmospheric energy cycle is examined using global analyses from the European Centre for Medium Range Weather Forecasts (ECMWF) for the period 1980–1987. Only January and July averages are considered.

It is confirmed that planetary stationary waves are basically baroclinic. Their contribution to the globally averaged energy cycle of the atmosphere is comparable to that of the transient waves. In January they contribute about 40% to the baroclinic conversion (CA) from zonal mean to eddy available potential energy. Local values for the northern hemisphere even show a predominant role of the stationary wave conversions over those originating from transient waves. Part of the available potential energy of stationary waves (A_{SE}) is converted to kinetic energy by warm air rising and cold air sinking. Nonlinear energy conversion, which can be interpreted as destruction of stationary temperature waves by transients, is the second sink for A_{SE}. The order of magnitude of these two processes is similar.

Barotropic nonlinear conversions, though negligible in the global average, reveal large conversion rates between the mean positions of the polar and the subtropical jets. Their orientation is suggestive of a tendency to increase stationary wave kinetic energy K_{SE} at its local minimum between the jets at the expense of the synoptic scale transients.

While all terms of the energy cycle related to stationary waves reveal a predominance of the planetary scale (zonal wave numbers 1–3) transient waves are governed by synoptic scale waves (zonal wave numbers 4–9) only with respect to the baroclinic and barotropic conversions: a significant amount of transient wave energy (50% for the global average of A_{TE}) is due to planetary scale waves.

1. Introduction

Both stationary (time mean) and transient (departure from time mean) atmospheric waves are a characteristic feature of the general circulation. The existence of the former is generally attributed to diabatic and orographic forcing. The relative importance of both types of forcing is still under debate (see e.g. Simmons, 1982; White, 1982; Wallace, 1983; Held, 1983; Hayashi and Golder, 1983; Heckley and Gill, 1984; Jacqmin and Lindzen, 1985; Nigam et al., 1986; Galin and Kirichkov, 1986; Blackmon et al., 1987; Fleming et al., 1987). Transient waves are understood as the result of baroclinic instability of the zonal mean flow. It was shown both in numerical experiments (e.g. Simmons and Hoskins, 1978, 1980; Held and Hoskins, 1985) and observations (e.g. Randel and Stanford, 1985 a, b) that the transient waves, particularly those related to the synoptic-scale, undergo a life-cycle. This life-cycle can most easily be understood in terms of the energy cycle proposed by Lorenz (1955): A phase of baroclinic growth, in which zonal available potential energy (AZ) is converted to eddy available potential energy (AE) predominantly by horizontal heat transports, is almost instantaneously followed by a conversion of AE to eddy kinetic energy by warm air rising and cold air sinking (Stein, 1986; Huang

and Vincent, 1988). This process is also called baroclinic. Later, the wave undergoes a phase of barotropic decay, when horizontal transports of momentum transfer energy from the wave to the zonal mean flow (*KZ*).

Energy conversions corresponding to this cycle have also been observed for the predominantly planetary-scale stationary waves (Holopainen, 1970; Lau and Oort, 1982), though these waves appear to be less efficient in converting available potential energy and kinetic energy when taking into account the size of the energy-reservoirs (Chen, 1982).

Linear (wave-zonal mean) energy conversions by transient and stationary waves are not independent from each other but (as one would expect from the baroclinic adjustment theory proposed by Stone, 1978) mutually influence their strength in different latitudes (van Loon, 1979; Rosen and Salstein, 1982). Meridional fluxes of sensible heat due to stationary waves reduce the baroclinicity of the mean zonal flow and thus reduce the necessity for fluxes due to the transients, and vice versa.

Besides the linear interactions there are also nonlinear interactions of both kinds of waves, which do not only appear to be important for "blocking" (see e.g. Hansen and Sutera, 1984; Ponater, 1985; Metz, 1986; Kung and Baker, 1986; Holopainen and Fortelius, 1987) but which, as Opsteegh and Vernekar (1982) demonstrated using a primitive equation model, are essential to obtain the correct positioning of the stationary waves of the northern hemisphere. Lau and Oort (1982) looked upon these nonlinear interactions from an energetical viewpoint. Their result for the northern hemisphere was that in winter transient eddies damp stationary temperature waves by transporting heat down the local temperature gradient. This process is, in the global integral, equivalent to a transfer of available potential energy from the stationary to the transient wave part of this reservoir. According to Lau and Oort, nonlinear interactions between transient and stationary waves of kinetic energy give low transformation rates when integrated hemispherically. However, the low value obtained is the result of large local contributions of opposite sign, thus leading to uncertainty about the sign of the global value.

The investigations mentioned above only used hemispheric data from the real atmosphere or were based on numerical simulations. With the data available here (see section 3), It was possible to carry out global investigations and interhemispheric comparisons. The goal of our investigation is to check the above-mentioned results with a comparatively long dataset and to obtain a closer insight into the energy cycle of the atmosphere by addressing the following questions:

- How important are baroclinic stationary waves with respect to the global energy cycle? Are there indications for a different role of these waves on the two hemispheres?
- Can an association between the zonally averaged contribution to the different terms of the energy cycle be detected? Is such an association different for stationary and transient waves? What is the role of the nonlinear conversions?

2. Method

The framework of the classical energy cycle is well known. We expanded the formulation of Arpe et al. (1986) to be able to distinguish between stationary (monthly mean) and transient (departure from monthly mean) waves. This so-called "Mixed Space-Time Domain" formulation of the energy cycle (Oort, 1964) is illustrated in Fig. 1. Formulae used are depicted in the appendix. Generation terms and dissipation terms have been computed as residuals corresponding to the budget equations also shown in the appendix. The time derivations of the different reservoirs in these equations have been estimated using the reservoirs of the preced-

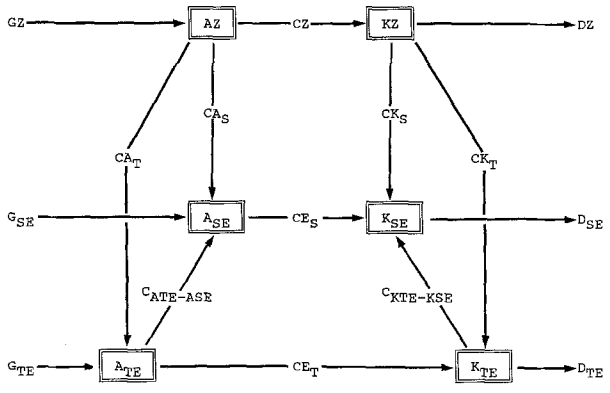

Fig. 1. Diagram of the global atmospheric energy cycle in the Mixed Space-Time Domain. Arrows indicate orientation of conversions corresponding to the definitions in the appendix

ing and of the following month, i.e. December and February for the January values, and June and August for the July values.

When considering the energy cycle for limited parts of the atmosphere, boundary fluxes would have to be computed. However, the local or zonally averaged integrands of the different terms generally indicate distinct physical processes or describe the state of the atmosphere. This is making them a useful tool for diagnosis of the atmospheric general circulation. For some of the terms of the energy cycle, like CE and the nonlinear conversions between stationary and transient waves, there are different possible formulations of the integrands (Ponater and Frenzen, 1988; Kung et al., 1983; Lau and Oort, 1982) which, of course, lead to different distributions of the integrand values. These distributions are associated with different physical aspects of the conversions, but should lead to the same global integrals. We will limit our investigation to the formulations noted in the Appendix.

Our approach to the energy cycle of stationary and transient waves will include a separation for waves of different zonal wave numbers. Long waves (zonal wave number 1–3), synoptic (wave number 4–9) and short scale waves (wave number 10–15) will be distinguished. Contribution of single wave numbers are not considered. Furthermore, no attempt is made to separate standing waves and travelling waves of different phase speed, which are all part of the transient waves. Generally, fast moving travelling waves are of synoptic or shorter scale in midlatitudes, while slowly moving ones are predominantly of planetary scale (e.g. Kung, 1988). An investigation of the energetics of the fast and slowly moving disturbances has been carried out by Sheng and Derome (1989).

3. Data

The data consist of 7 years of initialized global 00Z analyses of the ECMWF (1 dataset per day). The period covered is June 1980 to February 1987, but only January and July data are used for this study. Archived data consist of packed spherical harmonics of geopotential height, temperature, humidity, both horizontal wind components (or alternatively divergence and vorticity), and the vertical wind component for 13 pressure levels (1,000, 850, 700, 500, 400, 300, 250, 200, 150, 100, 70, 50, 30 hPa). From these data Fourier coefficients are computed at 59 equidistant latitudes between 87°N and 87°S. The maximum resolution depends on the truncation of the archived spherical harmonics, which has been reduced from T80 to T63 (triangular truncation) after April 20, 1983. While the changes in the archiving system (Arpe et al., 1986) are of no relevance to the results of our investigation, there have been several changes to the analysis procedure at ECMWF which clearly have an impact on the basic analysis-data itself. Of these changes (see Arpe et al., 1986; Trenberth and Olson, 1988 a, c for a listing) the major ones are those of the forecast model (altering the "first guess"), of the assimilation scheme (Rosen et al., 1985) and of the initialization (Trenberth, 1987). Arpe et al. (1986) suspected that these changes are relevant to some terms of the energy cycle, for example that they might be the cause of an observed trend for the term *CE*.

Considerable progress has been made in obtaining better values for upper air data over the southern hemisphere and the tropics. Still there remains some uncertainty on the analysis data for these areas arising from comparisons of different data sets (Heckley, 1985; Rosen et al., 1987; Trenberth and Olson, 1988 b).

We believe that, in spite of the above-mentioned uncertainties, the time averages for the different terms of the energy cycle presented below are a good estimate of these processes in the real atmosphere.

4. Results

4.1. The Global Energy Cycle

The globally averaged energy cycle as depicted in Fig. 1 is shown in Fig. 2 for January and Fig. 3 for July. Results agree well with observational estimates of the global energy cycle carried out by Kung and Tanaka (1983) for the FGGE Special Observation Periods. The data used here are, to a major part, identical to those used by Arpe et al. (1986); thus, their results for the space-domain energetics can be compared to the present results by adding our stationary and transient components of the different reservoirs and conversion terms. From the distinction between these two components it becomes clear that the stationary

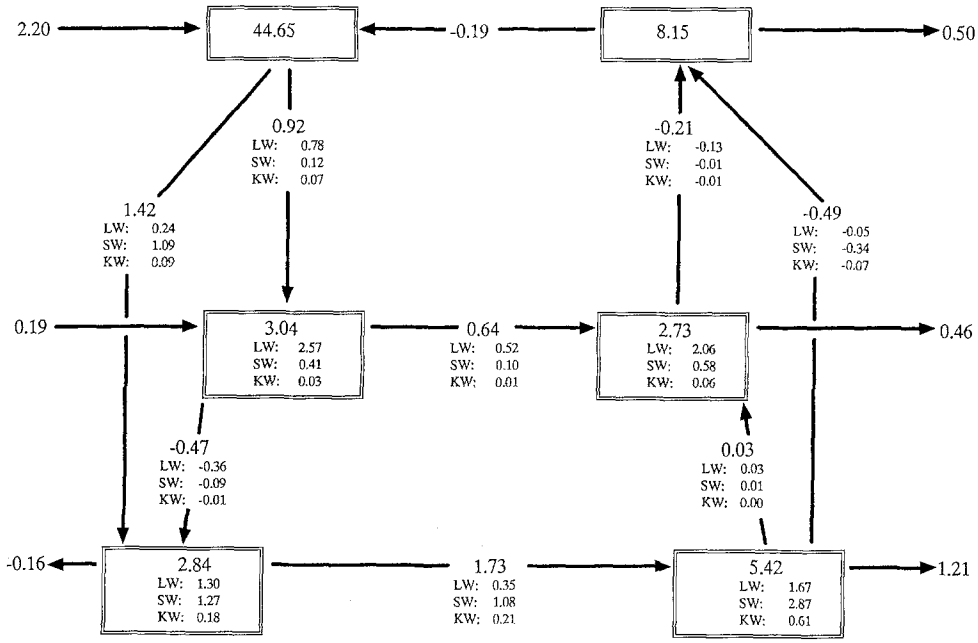

Fig. 2. The global atmospheric energy cycle for January, from ECMWF analyses 1981–1987. Reservoirs (in boxes) in J/(m^2*Pa). Conversions in W/m^2, with arrows indicating the observed orientation of conversions. *LW*, *SW*, and *KW* indicate the role of long (zonal wave number 1–3), synoptic scale (zonal wave number 4–9) and short waves (zonal wave number 10–15), respectively. For the nonlinear conversions $C_{ATE\text{-}ASE}$ and $C_{KTE\text{-}KSE}$ this separation only applies to the stationary waves, while all transient waves are included

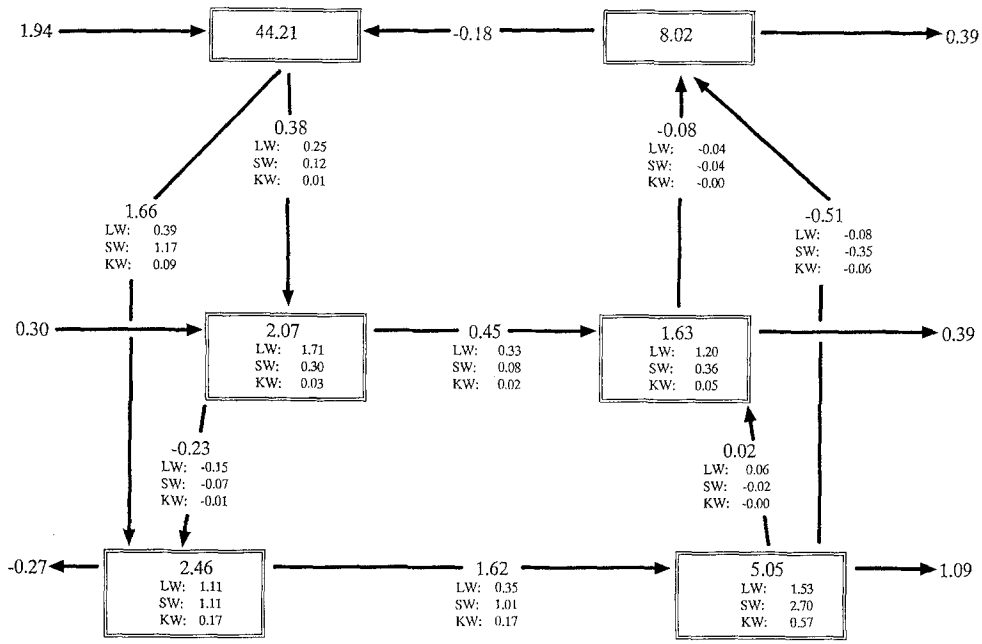

Fig. 3. As in Fig. 2 but for July, from ECMWF analyses 1980–1986

waves cannot be neglected compared with the transient ones. This holds for the reservoirs of available potential energy and kinetic energy as well as for the baroclinic and barotropic conversions *CA*, *CE*, and *CK*. With stationary waves being of maximum importance in northern hemisphere winter (e.g. Wallace, 1983), energies and conversion rates for the stationary waves for January exceed the corresponding ones for July by between 50% (A_{SE}, CE_S) and 100% or more (CA_S,

CK_S). Long waves of zonal wave number 1–3 clearly dominate all terms of the stationary subcycle (CA_S, A_{SE}, CE_S, K_{SE}, CK_S). The result for the transient subcycle is not quite as simple: While conversions are governed by synoptic scale waves, long transient waves contribute as much to the reservoir of A_{TE} as the synoptic scale transients. Long transient waves also play an important role in the reservoir of K_{TE}.

One might suspect that this relation between conversions and reservoirs is caused by the nonlinear conversion terms interconnecting the stationary and transient parts of the cycle. Indeed, while there is almost no global net conversion between the two eddy kinetic energy reservoirs, the conversion $C_{ATE\text{-}ASE}$ is playing an important role whithin the global energy cycle. It is directed from the stationary wave reservoir to the transient wave reservoir of available potential energy reaching the same order of magnitude as the baroclinic conversions of the stationary waves, CA_S and CE_S. Obviously the damping of stationary temperature waves by horizontal transient fluxes of sensible heat is an important process in the atmosphere, even when global and temporal averages are considered.

In Fig. 2 and 3 the separation into the different wave number groups is done with respect to the wave numbers of the stationary waves for the nonlinear conversions. The result of this separation is a clear dominance of the long stationary waves within $C_{ATE\text{-}ASE}$, which is consistent with the dominance of long waves in A_{SE}. As the nonlinear terms are determined by both stationary and transient waves (see formulae in the appendix) the question arises, if there is a similar dominance of a wave number group with respect to the transient waves, or if both are equally important. The latter would be consistent with the part of A_{TE} due to long and synoptic scale waves almost being equal. Our approach to this problem is to compute the nonlinear conversions without any long (zonal wave number 1–3) or without any shorter transient components (zonal wave number greater than 3), respectively. The result (not shown in Fig. 2 or 3) is that long and shorter transient waves contribute about equally to stationary wave damping. The conversion rate for $C_{ATE\text{-}ASE}$ in January is $-0.47\,W/m^2$ when all transient waves are considered, compared with $-0.17\,W/m^2$ when only long transient waves are used and $-0.18\,W/m^2$ for shorter (wave number 4 and higher) waves (not shown in Fig. 2). For July these values are $-0.23\,W/m^2$ (total), $-0.07\,W/m^2$ (long transient) and $-0.11\,W/m^2$ (short transient).

It should be noted at this point that adding the conversion rates computed using only long or shorter transient waves one does not end up with the result obtained when using all transient waves. This is due to the transient-transient correlations involved (see appendix). The physical background is that part of the total nonlinear conversion may be due to a combined action of planetary scale and shorter scale transient waves, e.g. a transient planetary wave of the temperature field interacting with a short scale "wave" in the meridional wind field. Such interactions have been left unconsidered in the previous computations.

4.2. Zonally Averaged Cross-Sections and Local Values

The results for the global integrals listed in the previous section give an impression of how the global energy cycle is working. They are also useful for comparison with results from other data sources for the observed atmosphere and with results from other GCMs. However, they tell only little about the physical background and the interrelations of the terms of the energy cycle. More insight can be gained from zonally averaged and local values, a number of which will be investigated below.

In this section, baroclinic conversions and available potential energy on the one hand and barotropic conversions and kinetic energy on the other hand are treated separately. The background of this is the lack of local interrelations between the baroclinic conversions CE_S and CE_T and the kinetic energy reservoirs K_{SE} and K_{TE}. The lack of such interrelations corresponds to the results of Baker and Brin (1985) who found that flux convergences of geopotential height are the most important source for local kinetic energy.

4.2.1. Available Potential Energy and Baroclinic Conversions

To investigate and compare details of the processes associated with baroclinic conversions of stationary and transient waves we start with a

comparison of the energy of the reservoirs A_{SE} and A_{TE} in the two months considered. For January these zonally averaged energies are shown in Fig. 4. As expected the largest tropospheric contributions to A_{SE} occur over northern hemisphere midlatitudes. The maximum is located at 45°N. The northern hemisphere maximum for the transient waves is located farther poleward (Fig. 4, bottom), with synoptic scale waves dominating between 35°N and 60°N and waves of zonal wave number 1–3 between 60°N and 80°N (not shown). This change in dominant wave number may be associated with the convergence of meridians and not with a change of the horizontal scale. Maximum energy of A_{SE} exceeds those of A_{TE} by more than 50%. Stratospheric energy is clearly dominated by the stationary waves. Transient contributions in this area are, as for the stationary part, almost exclusively of planetary scale. In the southern hemisphere, large values for A_{SE} are only observed over Antarctica. Part of this area of maximum values is not observed but is the result of extrapolation to pressure levels below ground. A_{TE} values are lower than their northern hemispheric counterparts. As in the northern hemisphere, synoptic scale waves dominate in midlatitudes, while high latitudes are dominated by low zonal wave numbers.

In contrast to A_{TE}, which is revealing almost the same structure in July as in January, the maximum values of A_{SE} for July are still found over the northern hemisphere (with the exception of Antarctica), but concentrated to the lowest part of the atmosphere between 20°N and 60°N and to a location between 20°N and 40°N, 200 to 400 hPa (Fig. 5). Arpe et al. (1986) stated that the latter "spot" is not due to low static stability like proposed by Oriol (1982) but is determined by a wave number 1 temperature wave. This maximum of stationary wave available potential energy at low latitudes is not a unique feature in the northern hemisphere in July: A weak relative maximum is located at about the same distance from the equator in the southern hemisphere (Fig. 5, top); similar maxima are found in January (Fig. 4, top). It will be shown further below that these maxima are associated with linear conversions CA_S and CE_S.

It is generally accepted that transient waves are reducing the meridional temperature gradient, predominantly by meridional transports of sensible heat. In terms of the energy cycle this process is described by the conversion CA_T, transferring energy from zonal (AZ) to transient eddy available potential energy (A_{TE}). Zonally averaged contributions to this conversion term are determined by the meridional temperature gradient and, simultaneously, by the magnitude of the sensible heat transports. A comparison of zonally averaged contributions to CA_T (Figs. 6 and 7, bottom) and A_{TE} (Figs. 4 and 5, bottom) reveals coincidence of maxima of energy values and conversion rates. An exception to this is found in January, when the northern hemisphere maximum of A_{TE} is much

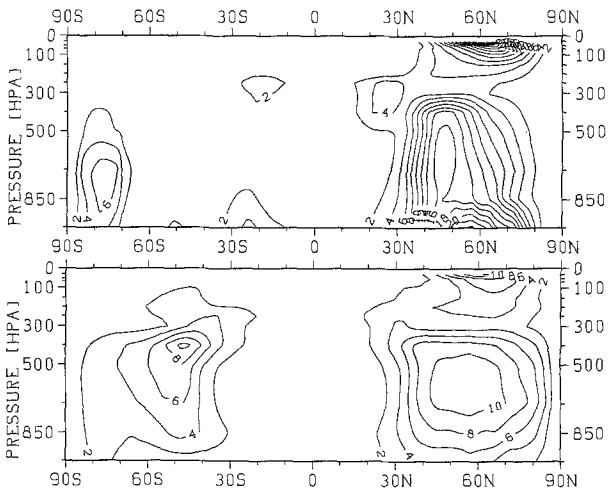

Fig. 4. Available potential energy of the stationary waves (A_{SE}, top) and of the transient waves (A_{TE}, bottom) in J/(m²*Pa), January

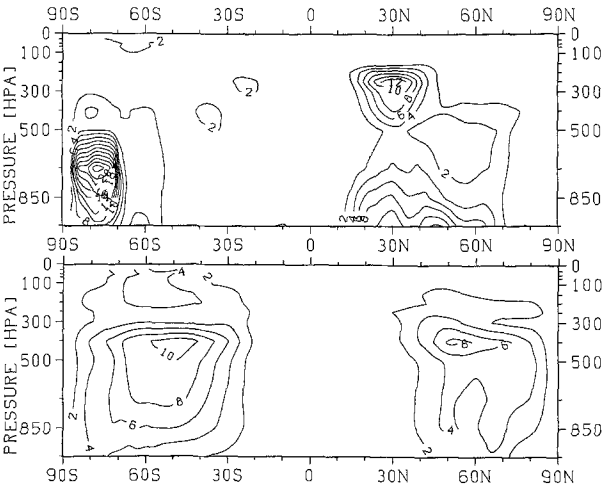

Fig. 5. Available potential energy of the stationary waves (A_{SE}, top) and of the transient waves (A_{TE}, bottom) in J/(m²*Pa), July

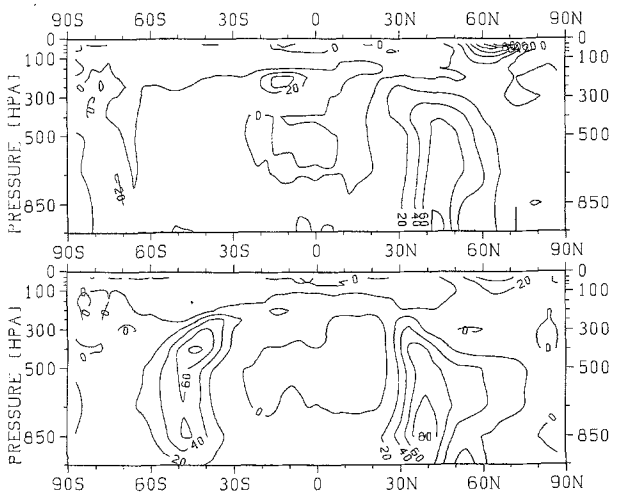

Fig. 6. Conversions CA_S (top) and CA_T (bottom) in 10^{-6} W/(m^2*Pa), January

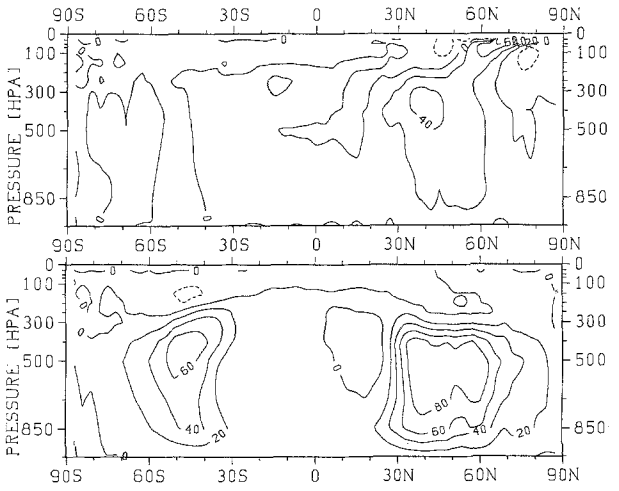

Fig. 8. Conversions CE_S (top) and CE_T (bottom) in 10^{-6} W/(m^2*Pa), January

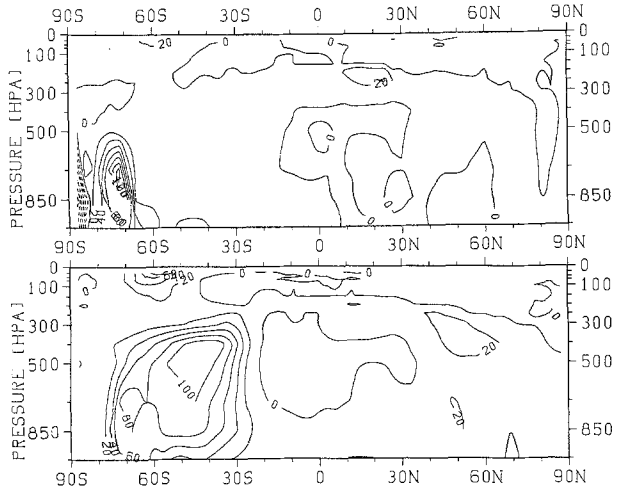

Fig. 7. Conversions CA_S (top) and CA_T (bottom) in 10^{-6} W/(m^2*Pa), July

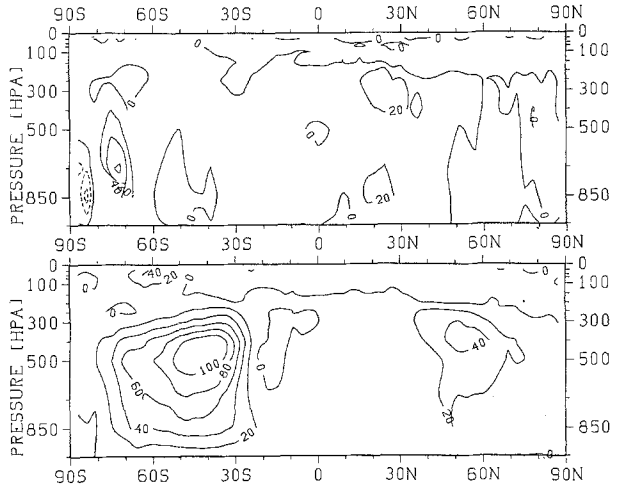

Fig. 9. Conversions CE_S (top) and CE_T (bottom) in 10^{-6} W/(m^2*Pa), July

farther northward than the maximum of CA_T. The northward extension of the reservoir was found to be due to intense "long" transient waves, but there is no associated maximum of CA_T. The coincidence for CA_S (Figs. 6 and 7, top) and A_{SE} (Figs. 4 and 5, top) is found to be very similar to that observed for the transient waves with respect to mid-tropospheric values. We consider this an indication of baroclinic processes associated with stationary waves comparable to those associated with transient waves.

Warm air rising and cold air sinking, equivalent to a conversion from available potential energy to kinetic energy and quantitatively described by CE_S and CE_T (Figs. 8 and 9), is observed with almost the same structure of zonally averaged contributions in the troposphere as the parent reservoirs. This even holds for the A_{TE} low zonal wave number maximum in northern hemisphere winter. However, conversion rates due to these "long" transient waves are small compared to synoptic scale wave conversions. This result is not unexpected in the light of the global integral results discussed previously.

A special note should be given about the locations of the observed "spots" of A_{SE} around 30°. Maxima of conversion rates CA_S and CE_S can indeed be found in the vicinity of the maxima of

A_{SE}. The relative maximum of A_{SE} around 20°S, 250 hPa in January (Fig. 4, top) corresponds to large conversion rates maximizing at 15°S immediately equatorward (Fig. 8, top). The same coincidence can be seen for the 30°N maximum of A_{SE} at the same level, where conversion rates are relatively large at its northern end. For July the conversions associated with the high energy at this latitude are found near 20°N. These baroclinic conversions at low latitudes are only due to vertical heat transports, i.e. horizontal transports do not give any significant contribution to CA_S (compare formula in the appendix). In an investigation for FGGE SOP-1 Huang and Vincent (1985) also found a maximum in stationary wave conversion CE_S, which was associated with the South Pacific Conversion Zone (0°–30°S). Contrary to our results, they did not find similar conversion rates for CA_S, which is probably due to different definitions of the stability-parameter.

Large values of A_{SE} near the surface observed between 10°N and 70°N in July (Fig. 5) are not associated with a CA_S maximum. The vertical decrease of energy suggests that these structures are governed by diabatic effects. One might tentatively associate the high globally averaged values of G_{SE} in July compared to January with this energy maximum.

Nonlinear stationary-transient energy conversions between A_{SE} and A_{TE} support the hypothesis of local (zonally averaged) interdependence between different parameters of the energy cycle almost perfectly. Their maximum contributions to the global integral are found between 40°N and 70°N in January (Fig. 10). This is the area where the high values of A_{TE} due to "long" zonal waves do not coincide with large conversion rates of CA_T. It appears that at these latitudes the predominant energy conversion is not from the zonal reservoir AZ but from the stationary wave reservoir, i.e. by nonlinear interactions. Further support for this hypothesis is given by a computation of $C_{ATE\text{-}ASE}$ using transient waves of wave number 1–3 only, confirming that these waves are the predominant contributor to the maximum of nonlinear conversions. Without inclusion of the nonlinear interactions between stationary and transient waves, the idea of interdependence of conversions and reservoirs in the zonal averages would be incomplete.

Apart from this maximum of negative values of $C_{ATE\text{-}ASE}$, low negative conversion rates are observed all over the troposphere. In January there is also a maximum of conversions from A_{SE} to A_{TE} in the stratosphere immediately over the north pole (Fig. 10), apparently associated with the high energy values a few degrees south (Fig. 4). Stratospheric energy values for the winter hemisphere are much smaller in July (Fig. 5), and as expected there is no local maximum of the nonlinear conversion. In July large values of $C_{ATE\text{-}ASE}$ are observed over Antarctica only (not shown). The upper troposphere maximum of A_{SE} at 30°N (Fig. 5, top) is not associated with strong nonlinear interactions. Still, as in January, negative values are observed throughout the troposphere, showing

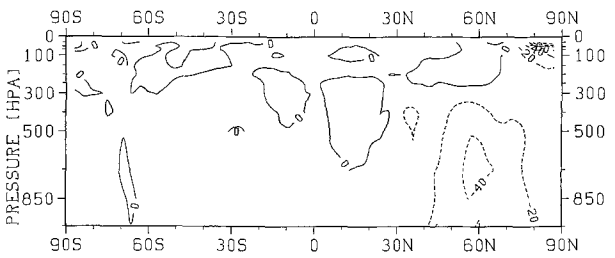

Fig. 10. Conversion $C_{ATE\text{-}ASE}$ ($A_{TE} \rightarrow A_{SE}$) in 10^{-6} W/(m^2*Pa), January

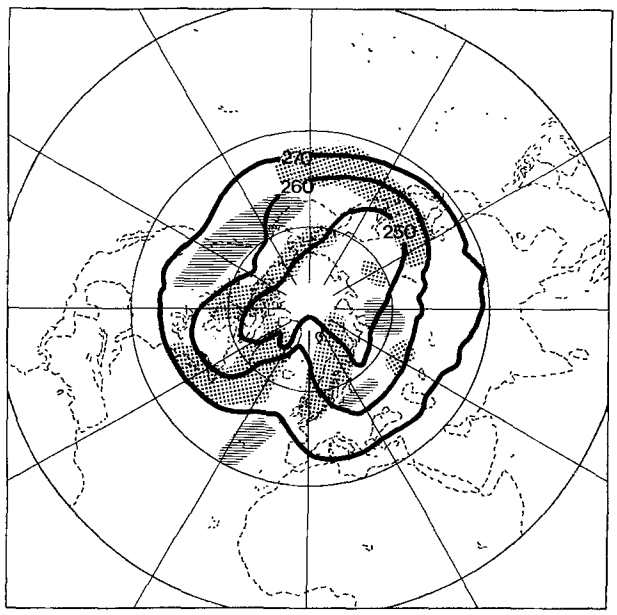

Fig. 11. Temperature in January 1987, 700 hPa, in K (ECMWF analyses). Shaded areas depict local contributions to $C_{ATE\text{-}ASE}$ greater than $50*10^{-6}$ W/(m^2*Pa) (dashed) and lower than $-50*10^{-6}$ W/(m^2*Pa) (stippled)

that destruction of stationary temperature waves by transients is a process not limited to distinct areas.

Looking at the northern hemispheric horizontal contributions to this term for the 700 hPa-level (Fig. 11) (chosen because of its maximum zonally averaged values in Fig. 10), it is possible to gain some insight into the processes leading to the zonally averaged structure. Local regions of positive and negative values are found, coinciding with regions of relatively warm (eastern parts of the oceans) and cold air, repectively. This structure can easily be understood considering the horizontal heat transports by the transient waves (see, e.g. Lau and Oort, 1982, their Fig. 10 or Kushnir and Esbensen, 1986, their Fig. 1 c). Heat is transported against the local temperature gradient by transient waves. Because of the prevailance of the meridional component of this gradient over the component of the gradient associated with the stationary waves, heat transports are predominantly directed towards the pole. Poleward heat transports against the zonal mean temperature gradient are contributing to CA_T. With respect to $C_{ATE\text{-}ASE}$ they lead to the positive and negative contributions observed in Fig. 11, positive if this heat transport is directed into relatively warm regions, negative if it is directed into relatively cold ones.

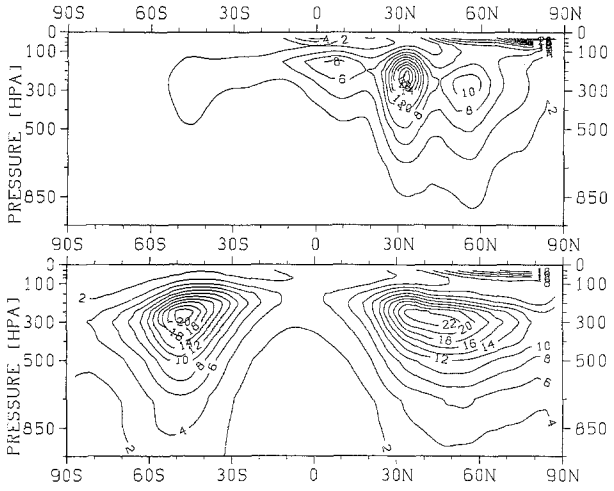

Fig. 12. Kinetic energy of the stationary waves (K_{SE}, top) and of the transient waves (K_{TE}, bottom) in J/(m^2*Pa), January

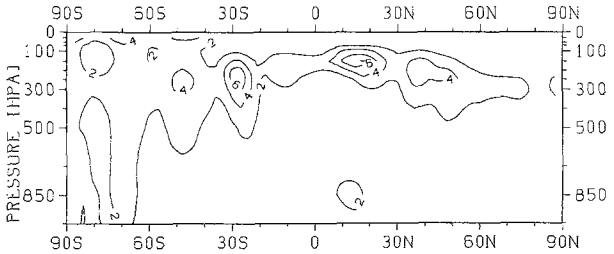

Fig. 13. Kinetic energy of the stationary waves (K_{SE}) in J/(m^2*Pa), July

4.2.2. Kinetic Energy and Barotropic Conversions

For January, analyses show an intense maximum of stationary eddy kinetic energy at 30°N, 200 hPa (Fig. 12, top) associated with the zonal wind speed maximum of the subtropical jet. Minor maxima are found near the equator and at 55°N. We associate the latter with the polar jet. The high stratospheric values of K_{SE} correspond to the polar night jet. While for K_{SE} there is a relative minimum between the polar and subtropical jet maximum, K_{TE} (Fig. 12, bottom) shows a broad area of high values. There are also large K_{TE} values associated with the southern hemisphere subtropical jet and the northern hemispheric polar night jet. As for A_{TE}, polar and stratospheric waves of K_{TE} are predominantly of planetary scale.

For July, the distribution of K_{TE} is very similar to that in January, except that the maxima are displaced northward by some 10° in both hemispheres (not shown). For the stationary wave part (K_{SE}) the energy distribution looks very different: A band of high values is observed at the tropopause level almost over the entire globe (Fig. 13). Comparatively weak maxima are observed at the location of the zonal mean jets (30°S, 45°N) and at 15°N. Another maximum is found where one would except the polar jet according to the January results. However, no distinct maximum of K_{SE} is found at the location of the polar night jet at 60°S. In contrast to the northern winter situation this jet is almost perfectly zonal (reservoir KZ not shown) with a small transient wave component.

The zonally averaged contributions of the nonlinear conversion $C_{KTE\text{-}KSE}$ between stationary and transient waves of kinetic energy show only one strong positive maximum in January (Fig. 14). Comparing its location with respect to the zonally averaged values of K_{SE} (Fig. 12), it is found that this maximum of the nonlinear conversion

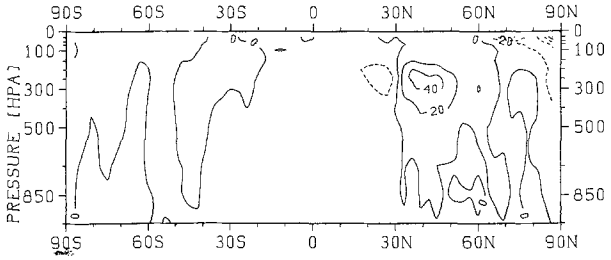

Fig. 14. Conversion $C_{KTE\text{-}KSE}$ ($K_{TE} \rightarrow K_{SE}$) in 10^{-6} W/(m^2*Pa), January

$C_{KTE\text{-}KSE}$ is placed between the two maxima of K_{SE} which we had assigned to polar and subtropical jet previously. With over $40*10^{-6}$ W/(m^2*Pa) in January and over $20*10^{-6}$ W/(m^2*Pa) in July these zonally averaged values are of the same order of magnitude as the local contributions to the linear conversion CK_S (not shown). The fact that these conversions are found where K_{SE} is at a local minimum and K_{TE} is at a maximum can be considered an indication of a physical mechanism forcing the atmosphere to a more uniform state. Indeed, the time series of zonally and vertically averaged K_{SE} (not shown) indicates that separate strong maxima for polar and subtropical jet are only found for one or two months during northern winter. The hypothesis of such a mechanism is further supported by the fact that the positive (from transient to stationary) maximum of $C_{KTE\text{-}KSE}$ is only due to shorter (wave number greater than 3) transients, which indeed dominate K_{TE} at this latitude, interacting with planetary stationary waves which dominate K_{SE}. As it is suggested by the global integral values considered in the previous section, the result is different when long transient waves within this interaction are the only ones used for computation. These waves are extracting energy from the stationary waves over the entire atmosphere, with maximum conversion rates observed in the tropics. Thus, the effect of long transient waves on long stationary waves is similar in both nonlinear stationary-transient interactions for available potential energy and for kinetic energy.

Local northern hemispheric values of this nonlinear conversion are depicted in Fig. 15 for January 1987, 200 hPa. Positive values are found downstream of the jet maxima over the Atlantic and the Pacific ocean, while negative values prevail over the jet entrance regions. The distribution of

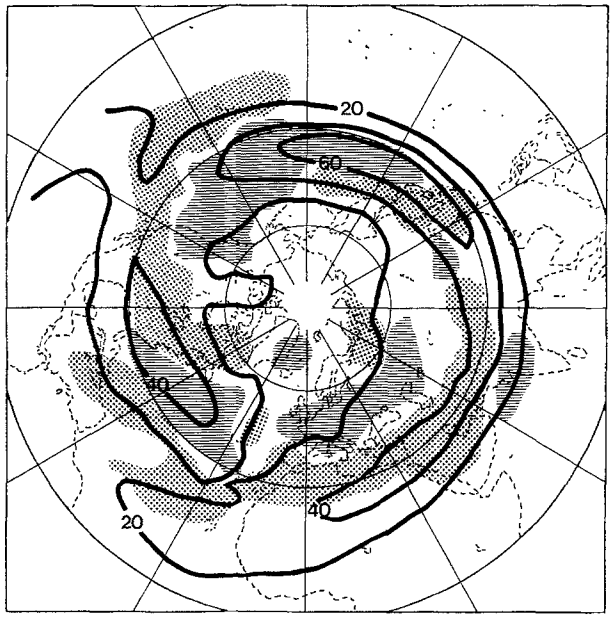

Fig. 15. Wind velocity in January 1987, 200 hPa, in m/s (ECMWF analyses). Shaded areas depict local contributions to $C_{KTE\text{-}KSE}$ greater than $50*10^{-6}$ W/(m^2*Pa) (dashed) and lower than $-50*10^{-6}$ W/(m^2*Pa) (stippled)

positive and negative local values is consistent with results obtained by Hoskins et al. (1983) and Wallace and Lau (1985) using the E-vector method. They find "a tendency of the transient eddies to extend the strong westerly flow further across the Atlantic" (Hoskins et al., 1983), and a similar pattern associated with the Pacific storm track. Such a tendency can be interpreted as a "strenghtening" of stationary waves if westerly forcing takes place where westerly flow is comparatively intense, i.e. close to the local jet maxima, while it means weakening of stationary waves if it occurs close to local minima of the westerly flow. Thus, both their and our results support the idea of nonlinear stationary-transient interactions are strengthening stationary waves in the areas east of the continents. However, positive and negative contributions lead to a zero net conversion in the zonal average for 30°N (Fig. 14), while apparently the positive zonal mean values north of this latitude (Fig. 14) are associated with a poleward bend of the areas with positive signature (Fig. 15).

5. Concluding Remarks

An investigation on the atmospheric energy cycle was carried out with special respect to the role of

stationary and transient waves ("Mixed Space-Time Domain"). We found significant contributions to all terms of the globally averaged energy cycle due to stationary waves. Their zonally averaged contributions even exceed those of the transient waves in northern hemisphere winter (January). Intense stationary waves in the southern hemisphere are only found near Antarctica. Conversions and reservoirs associated with stationary waves are governed by planetary scale waves (zonal wave number 1–3). The assumption that the terms of the energy cycle associated with transient waves are dominated by synoptic scale waves only holds for the conversions. Planetary scale transients are an important part of the reservoirs of K_{TE} and A_{TE}, even contributing some 50% to A_{TE}. Part of the relative importance of these waves in the reservoirs compared to the conversions may be due to the nonlinear stationary-transient conversions. The conversion from A_{SE} to A_{TE} proved to be large even when the global average was considered, while globally averaged conversion rates for $C_{KTE\text{-}KSE}$ are about zero.

A closer look at the role of transient waves of different wave number within the nonlinear conversions revealed that about half of the conversion $C_{ARE\text{-}ASE}$ is due to the planetary scale waves, half due to the shorter scale transients. This is, indeed, the relation of the different scales in the reservoir A_{TE}. Such a coincidence is not found for kinetic energy: while long transient waves extract energy from the reservoir K_{SE}, the opposite orientation of this conversion is observed when transient waves shorter than zonal wave number 3 are considered. Comparable effects have also been found by Holopainen et al. (1988) in the context of transient eddy geopotential tendencies.

We believe that conversions due to nonlinear stationary-transient interactions are not sufficient to explain the discrepancy between conversions and reservoirs with respect to long transient waves. Another possible cause that is to be ruled out is the nonlinear interaction between different wave numbers within the transient wave reservoirs. Lambert (1987), Kung and Tanaka (1983) and Chen (1982) all found fluxes from long waves to shorter scale waves of available potential energy due to nonlinear energy conversions. On the other hand, these investigations give some indication for energy flow from shorter to long waves of kinetic energy. One might suggest that normal modes of the atmosphere (e.g. external Rossby waves) are a major part of the transient long waves of available potential energy and kinetic energy. The dominant modes are travelling (consequently transient) waves of planetary scale. Tanaka (1985) and Kung and Tanaka (1988) carried out a three-dimensional normal mode energetics analysis for the FGGE year. They found about as much energy in the barotropic mode (vertical index zero) as in the baroclinic modes when kinetic energy is concerned, while for available potential energy the energy is almost completely contained in the baroclinic modes. It is not possible to compute explicitly the baroclinic conversion from available potential energy to kinetic energy using their scheme. Thus normal modes remain a possible background for the observed association of high energies and low conversion rates for low zonal wave numbers.

Looking at latitude-height distributins for conversions and reservoirs, we found evidence of interdependence of zonally averaged values of the different terms of the energy cycle both for stationary and transient waves. In most cases, conversions and reservoirs had maxima at the same latitude and height or immediately adjacent. A very instructive example is found in January, when the northern hemisphere maximum of A_{TE} is only partly coinciding with the linear conversion CA_T. In high latitudes, where no coincidence between this conversion and this reservoir is found, maximum values of the nonlinear conversion $C_{ATE\text{-}ASE}$ are found. Apart from its numerical value, this clearly displays the importance of this nonlinear term. Though the global integral for the other nonlinear term, $C_{KTE\text{-}KSE}$, vanishes, there appears to be a significant local physical effect. We argued that the atmosphere tends to come to a more uniform state filling the minimum of K_{SE} between the subtropical and the polar jet by a transfer from the transient eddy kinetic energy reservoir, which has its maximum at this place.

Appendix

List of Symbols, Definitions and Abbreviations

c_p = specific heat at constant pressure
g = gravity of earth
p = pressure
r = radius of earth
R = gas constant
t = time
T = temperature

T_V = virtual temperature
u = zonal wind
v = meridional wind
ω = vertical p-velocity
φ = latitude
λ = longitude
γ = stability parameter

$$= -\frac{R}{p}\left(\frac{\partial}{\partial p}[\overline{T}] - \frac{R}{c_p}\frac{[\overline{T}]}{p}\right)^{-1}$$

$\overline{x}$ = time mean of x (stationary part)
x' = deviation from time mean (transient part)
$\{x\}$ = global horizontal mean
$[x]$ = zonal mean
x^* = deviation from zonal mean

AZ = zonal available potential energy

$$= \frac{\gamma}{2g}([\overline{T}] - \{\overline{T}\})^2$$

AE = eddy available potential energy = $A_{SE} + A_{TE}$
A_{SE} = stationary eddy available potential energy

$$= \frac{\gamma}{2g}[\overline{T^{*2}}]$$

A_{TE} = transient eddy available potential energy

$$= \frac{\gamma}{2g}[\overline{T'^2}]$$

KZ = zonal kinetic energy

$$= \frac{1}{2g}([\overline{u}]^2 + [\overline{v}]^2)$$

KE = eddy kinetic energy = $K_{SE} + K_{TE}$
K_{SE} = stationary eddy kinetic energy

$$= \frac{1}{2g}[\overline{u^{*2}} + \overline{v^{*2}}]$$

K_{TE} = transient eddy kinetic energy

$$= \frac{1}{2g}[\overline{u'^2} + \overline{v'^2}]$$

CA = conversion from AZ to AE
CA_S = conversion from AZ to A_{SE}

$$= -\frac{\gamma}{g}\left([\overline{v}^*\overline{T}^*]\frac{\partial[\overline{T}]}{r\,\partial\varphi} + [\overline{\omega}^*\overline{T}^*]\left(\frac{\partial}{\partial p}([\overline{T}] - \{\overline{T}\}) - \frac{R}{p\cdot c_p}([\overline{T}] - \{\overline{T}\})\right)\right)$$

CA_T = conversion from AZ to A_{TE}

$$= -\frac{\gamma}{g}\left([\overline{v'T'}]\frac{\partial[\overline{T}]}{r\,\partial\varphi} + [\overline{\omega'T'}]\left(\frac{\partial}{\partial p}([\overline{T}] - \{\overline{T}\}) - \frac{R}{p\cdot c_p}([\overline{T}] - \{\overline{T}\})\right)\right)$$

CZ = conversion from AZ to KZ

$$= -([\overline{\omega}] - \{\overline{\omega}\})([\overline{T}_v] - \{\overline{T}_v\})\frac{R}{g\cdot p}$$

CE = conversion from AE to KE

CE_S = conversion from A_{SE} to K_{SE}

$$= -[\overline{\omega}^*\overline{T}_v^*]\frac{R}{g\cdot p}$$

CE_T = conversion from A_{TE} to K^{TE}.

$$= -[\overline{\omega' T_v'}]\frac{R}{g\cdot p}$$

CK = conversion from KZ to KE
CK_S = conversion from KZ to K_{SE}

$$= -\frac{1}{g}\left([\overline{u}^*\overline{v}^*]\frac{\partial[\overline{u}]}{r\,\partial\varphi} + [\overline{u}^*\overline{v}^*]\cdot[\overline{u}]\frac{\mathrm{tg}\,\varphi}{r} + [\overline{v}^*\overline{v}^*]\frac{\partial[\overline{v}]}{r\,\partial\varphi} - [\overline{u}^*\overline{u}^*]\frac{\mathrm{tg}\,\varphi}{r}[\overline{v}] + [\overline{\omega}^*\overline{u}^*]\frac{\partial[\overline{u}]}{\partial p} + [\overline{\omega}^*\overline{v}^*]\frac{\partial[\overline{v}]}{\partial p}\right)$$

CK_T = conversion from KZ to K_{TE}

$$= -\frac{1}{g}\left([\overline{u'v'}]\frac{\partial[\overline{u}]}{r\,\partial\varphi} + [\overline{u'v'}]\cdot[\overline{u}]\frac{\mathrm{tg}\,\varphi}{r} + [\overline{v'v'}]\frac{\partial[\overline{v}]}{r\,\partial\varphi} - [\overline{u'u'}]\frac{\mathrm{tg}\,\varphi}{r}[\overline{v}] + [\overline{\omega'u'}]\frac{\partial[\overline{u}]}{\partial p} + [\overline{\omega'v'}]\frac{\partial[\overline{v}]}{\partial p}\right)$$

$C_{ATE\text{-}ASE}$ = conversion from A_{TE} to A_{SE}

$$= \frac{\gamma}{g}\left(\overline{u'T'}^*\frac{1}{r\cos\varphi}\frac{\partial\overline{T}^*}{\partial\lambda} + \overline{v'T'}^*\frac{\partial\overline{T}^*}{r\,\partial\varphi}\right)$$

$C_{KTE\text{-}KSE}$ = conversion from K_{TE} to K_{SE}

$$= \frac{1}{g}\left(\overline{u'u'}^*\frac{1}{r\cos\varphi}\frac{\partial\overline{u}^*}{\partial\lambda} + \overline{u'v'}^*\frac{\partial\overline{u}^*}{r\,\partial\varphi} + \overline{u'v'}^*\cdot\overline{u}^*\frac{\mathrm{tg}\,\varphi}{r} + \overline{v'v'}^*\frac{\partial\overline{v}^*}{\partial\varphi} - [\overline{u'u'}]^*\frac{\mathrm{tg}\,\varphi}{r}\overline{v}^* + \overline{u'v'}^*\frac{1}{r\cos\varphi}\frac{\partial\overline{v}^*}{\partial\lambda}\right)$$

GZ = generation of AZ
G_{SE} = generation of A_{SE}
G_{TE} = generation of A_{TE}
DZ = dissipation of KZ
D_{SE} = dissipation of K_{SE}
D_{TE} = dissipation of K_{TE}

Budget equations:

$$\frac{\partial AZ}{\partial t} = GZ - CA_S - CA_T - CZ$$

$$\frac{\partial A_{SE}}{\partial t} = G_{SE} + CA_S - CE_S + C_{ATE\text{-}ASE}$$

$$\frac{\partial A_{TE}}{\partial t} = G_{TE} + CA_T - CE_T - C_{ATE\text{-}ASE}$$

$$\frac{\partial K_{TE}}{\partial t} = -D_{TE} + CE_T + CK_T - C_{KTE\text{-}KSE}$$

$$\frac{\partial K_{SE}}{\partial t} = -D_{SE} + CE_S + CK_S + C_{KTE\text{-}KSE}$$

$$\frac{\partial KZ}{\partial t} = -DZ - CK_S - CK_T + CZ$$

Acknowledgements

We gratefully acknowledge the help of ECMWF and the German Weather Service (DWD) in providing us with the analysis data and with some computer programs that we could use as the basis for our programs. For the implementation at the Climate Computing Centre in Hamburg we got help from C. Brancovic of ECMWF, E. Kirk of the University of Hamburg, M. Barbulescu from our institute and several others. We wish to thank M. Ponater of the University of Hamburg for many discussions and comments. This work was supported by the Minister of Research of the Federal Republic of Germany within the Climate Research Program under grant 07KF2121.

References

Arpe, K., Brancovic, C., Oriol, E., Speth, P., 1986: Variability in time and space of energetics from a long series of atmospheric data produced by ECMWF. *Beitr. Phys. Atmos.*, **59**, 321–363.

Baker, W. E., Brin, Y., 1985: A comparison of observed and forecast energetics over North America. *Quart. J. Roy. Meteor. Soc.*, **111**, 641–355.

Blackmon, M. L., Branstator, G. W., Bates, G. T., Geisler, J. E., 1987: An analysis of equatorial Pacific sea surface temperature anomaly experiments in general circulation models with and without mountains. *J. Atmos. Sci.*, **44**, 1828–1844.

Chen, T.-C., 1982: A further study of spectral energetics in the winter atmosphere. *Mon. Wea. Rev.*, **110**, 947–961,

Fleming, E. L., Lim, G.-H., Wallace, J. M., 1987: Differences between the spring and autumn circulation of the Northern Hemisphere. *J. Atmos. Sci.*, **44**, 1266–1286.

Galin, M. B., Kirichkov, S. Y., 1986: Energetics of circulation states in a model including orography. *Izvestiya, Atmospheric and Oceanic Physics*, **22**, 613–619.

Hansen, A. R., Sutera, A., 1984: A comparison of the spectral energy and enstrophy budgets of blocking versus nonblocking periods. *Tellus*, **36A**, 52–63.

Hayashi, Y., Golder, D. G., 1983: Transient planetary waves simulated by GFDL spectral general circulation models. Part I: Effects of mountains. *J. Atmos. Sci.*, **40**, 941–950.

Heckley, W. A., 1985: Systematic errors of the ECMWF operational forecasting model in tropical regions. *Quart. J. Roy. Meteor. Soc.*, **111**, 709–738.

Heckley, W. A., Gill, A. E., 1984: Some simple analytical solutions to the problem of forced equatorial long waves. *Quart. J. Roy. Meteor. Soc.*, **110**, 203–217.

Held, I. M., 1983: Stationary and quasi-stationary eddies in the extratropical troposphere: theory. In: Hoskins, B. J., Pearce, R. P. (ed.) *Large-scale dynamical processes in the atmosphere*, London: Academic Press, pp. 127–168.

Held, I. M., Hoskins, B. J. 1985: Large-scale eddies and the general circulation of the troposphere. In: Manabe, S. (ed.) *Advances in geophysics*, **28A**, Issues in atmospheric and oceanic modeling. Climate Dynamics, Orlando: Academic Press, pp. 3–31.

Holopainen, E. O., 1970: An observational study of the energy balance of the stationary disturbances in the atmosphere. *Quart. J. Roy. Meteor. Soc.*, **96**, 626–644.

Holopainen, E., Fortelius, C., 1987: High-frequency transient eddies and blocking. *J. Atmos. Sci.*, **44**, 1632–1645.

Holopainen, E., Fortelius, C., Ruosteenoja, K., 1988: The effect of transient eddies on the stationary eddy isobaric height field. *J. Atmos. Sci.*, **45**, 1760–1769.

Hoskins, B. J., James, I. N., White, G. H., 1983: The shape, propagation and mean-flow interaction of large-scale weather systems. *J. Atmos. Sci.*, **40**, 1595–1612.

Huang, H.-J., Vincent, D. G., 1985: Significance of the South Pacific convergence zone in energy conversions of the southern hemisphere during FGGE, 10–27 January 1979. *Mon. Wea. Rev.*, **113**, 1359–1371.

Huang, H.-J., Vincent, D. G., 1988: Daily spectral energy conversions of the global circulation during 10–27 January 1979. *Tellus*, **40A**, 37–49.

Jacqmin, D., Lindzen, R. S., 1985: The causation and sensitivity of the northern winter planetary waves. *J. Atmos. Sci.*, **42**, 724–745.

Kung, E. C., 1988: Spectral energetics of the general circulation and time spectra of transient waves during the FGGE year. *J. Climate*, **1**, 5–19.

Kung, E. C., Baker, W. E., 1986: Spectral energetics of the observed and simulated northern hemisphere general circulation during blocking episodes. *J. Atmos. Sci.*, **43**, 2792–2812.

Kung, E. C., Masters, S. E., Corte-Real, J. A. M., 1983: Large-scale energy transformations in the high latitudes of the northern hemisphere. *J. Atmos. Sci.*, **40**, 1061–1072.

Kung, E. C., Tanaka, H., 1983: Energetics analysis of the global circulation during the Special Observation Periods of FGGE. *J. Atmos. Sci.*, **40**, 2575–2592.

Kushnir, Y., Esbensen, S. K., 1986: Northern hemisphere wintertime variability in a two-level general circulation model. Part II: The maintenance of short and long timescale disturbances. *J. Atmos. Sci.*, **43**, 2985–2998.

Lambert, S. J., 1987: Spectral energetics of the Canadian climate centre general circulation model. *Mon. Wea. Rev.*, **115**, 1295–1305.

Lau, N.-C., Oort A. H., 1982: A comparative study of observed northern hemisphere circulation statistics based on GFDL and NMC analyses. Part II: Transient eddy statistics and the energy cycle. *Mon. Wea. Rev.*, **110**, 889–906.

Van Loon, H., 1979: The association between latitudinal temperature gradient and eddy transport. Part I: Transport of sensible heat in winter. *Mon. Wea. Rev.*, **107**, 525–534.

Lorenz, N. L., 1955: Available potential energy and the maintenance of the general circulation. *Tellus*, **7**, 157–167.

Metz, W., 1986: Transient cyclone-scale vorticity forcing of blocking highs. *J. Atmos. Sci.*, **43**, 1467–1483.

Nigam, S., Held, I. M., Lyons, S. W., 1986: Linear simulation of stationary eddies in a general circulation model. Part I: The no-mountain model. *J. Atmos. Sci.*, **43**, 2944–2961.

Oort, A. H., 1964: On estimates of the atmospheric energy cycle. *Mon. Wea. Rev.*, **92**, 483–493.

Opsteegh, J. D., Vernekar, A. D., 1982: A simulation of the January standing wave pattern including the effects of transient eddies. *J. Atmos. Sci.*, **39**, 734–744.

Oriol, E., 1982: Energy budget calculations at ECMWF. Part

I: Analyses 1980–1981. ECMWF Tech. Rep. No. 35, 114 pp.

Ponater, M., 1985: Räumlich-zeitliche Entwicklung energetischer Parameter während blockierender Wetterlagen. Mitteilungen aus dem Institut für Geophysik und Meteorologie der Universität zu Köln, Heft 46.

Ponater, M., Frenzen, G., 1987: On the numerical evaluation of the energy conversion integral. *Tellus*, **39 A**, 515–520.

Randel, W. J., Stanford, J. L., 1985 a: An observational study of medium-scale wave dynamics in the Southern Hemisphere summer. Part I: Wave structure and energetics. *J. Atmos. Sci.*, **42**, 1172–1188.

Randel, W. J., Stanford, J. L., 1985 b: The observed life cycle of a baroclinic instability. *J. Atmos. Sci.*, **42**, 1364–1373.

Rosen, R. D., Salstein, D. A., 1982: General circulation statistics on short time scales. *Mon. Wea. Rev.*, **110**, 683–689.

Rosen, R. D., Salstein, D. A., Peixoto, J. P., Oort, A. H., Lau, N.-C., 1985: Circulation statistics derived from level III-b and station-based analyses during FGGE. *Mon. Wea. Rev.*, **113**, 65–88.

Rosen, R. D., Salstein, D. A., Miller, A. J., Arpe, K., 1987: Accuracy of atmospheric angular momentum estimates from operational analyses. *Mon. Wea. Rev.*, **115**, 1627–1639.

Sheng, J., Derome, J., 1989: Observed and simulated energy cycles in the frequency domain. IAMAP 89 Abstracts Vol. II, ND 17.

Simmons, A. J., 1982: The forcing of stationary wave motion by tropical diabatic heating. *Quart. J. Roy. Meteor. Soc.*, **108**, 503–534.

Simmons, A. J., Hoskins, B. J., 1978: The life cycles of some nonlinear baroclinic waves. *J. Atmos. Sci.*, **35**, 414–432.

Simmons, A. J., Hoskins, B. J., 1980: Barotropic influences on the growth and decay of nonlinear baroclinic waves. *J. Atmos. Sci.*, **37**, 1679–1684.

Stein, C., 1986: Das zeitliche Zusammenwirken barokliner Energieumwandlungen durch großräumige Wellen in der Atmosphäre. Diplomarbeit, Institut für Geophysik und Meteorologie der Universität zu Köln.

Stone, P. H., 1978: Baroclinic adjustment. *J. Atmos. Sci.*, **35**, 561–571.

Trenberth, K. E., 1987: The role of eddies in maintaining the westerlies in the southern hemisphere winter. *J. Atmos. Sci.*, **44**, 1498–1508.

Trenberth, K. E., Olson, J. G., 1988 a: ECMWF global analyses 1979–1986: Circulation statistics and data evaluation. NCAR Tech. Note NCAR/TN-300 + STR. 94 pp.

Trenberth, K. E., Olson, J. G., 1988 b: Intercomparison of NMC and ECMWF global analyses 1980–1986. NCAR Tech. Note NCAR/TN-301 + STR. 81 pp.

Trenberth, K. E., Olson, J. G., 1988 c: An evaluation and intercomparison of global analyses from the National Meteorological Center and the European Center for Medium Range Weather Forecasts. *Bull. Amer. Meteor. Soc.*, **69**, 1047–1057.

Wallace, J. M., 1983: The climatological mean stationary waves: observational evidence. In: Hoskins, B. J., Pearce, R. P. (ed.) Large-scale dynamical processes in the atmosphere, London: Academic Press, pp. 27–53.

Wallace, J. M., Lau, N.-C., 1985: On the role of barotropic energy conversions in the general circulation. In: Manabe, S. (ed.) *Advances in geophysics*, **28 A**, Issues in atmospheric and oceanic modeling, Climate Dynamics, Orlando: Academic Press, pp. 33–74.

White, G. H., 1982: An observational study of the Northern Hemisphere extratropical summertime general circulation. *J. Atmos. Sci.*, **39**, 24–40.

Authors' address: Dr. U. Ulbrich, Institut für Geophysik und Meteorologie, Universität zu Köln, Kerpener Str. 13, D-W-5000 Köln 41, Federal Republic of Germany.